Extension of the Z_{eff} Diagnostic at ASDEX Upgrade

H. Meister, J.C. Fuchs, B. Kurzan, K.H. Steuer and ASDEX Upgrade Team

Max-Planck-Institut für Plasmaphysik, EURATOM Assoziation
Boltzmannstr. 2, D-85748 Garching b. München

Introduction The study of the contamination of tokamak plasmas by impurities still remains an important aspect of fusion research as the performance of future burning plasma reactors will rely on maintaining a clean plasma with a modest effective ionic charge ($Z_{\text{eff}} \leq 1.9$). Furthermore the radial location of the impurities must be measured accurately in order to predict their effect on fusion performance, especially in the regimes of the "advanced tokamak" with their variety of high confinement modes, possible impurity accumulation and current profile control schemes.

A possible means to assess the radial Z_{eff}-profile is the measurement of the bremsstrahlung using several sight-lines. Up to now an array of 16 sight-lines with avalanche diodes from the vertical Thomson-scattering system (VTS) [1] has been used measuring at wavelengths between 1020nm and 1063nm. These sight-lines, viewing radially onto the inner heat shield, suffered in many cases from the observation of reflections and thermal radiation giving large error bars to the results. In order to provide reliable Z_{eff}-profiles, the extension of the diagnostic is underway and will be presented together with first results for typical ASDEX Upgrade plasma regimes.

Current diagnostic set-up

Up to now the Z_{eff} diagnostic at ASDEX Upgrade has been extended to altogether 57 sight-lines viewing in poloidal and toroidal directions. Figure 1 shows their projection into a poloidal cross-section of ASDEX Upgrade. The 16 sight-lines mentioned above have been supplemented by 6 sight-lines of the newly installed horizontal Thomson-scattering system (HTS). Both arrays are equipped with filters of varying width between 1020–1063 *nm* and avalanche-diodes as detectors. Another array of 35 sight-lines (ZEA) is arranged in a poloidal cross-section and equipped with a photodiode array and a filter restricting the observed wavelengths to the range of 535–540 *nm* and thus reducing the amount of observed thermal radiation.

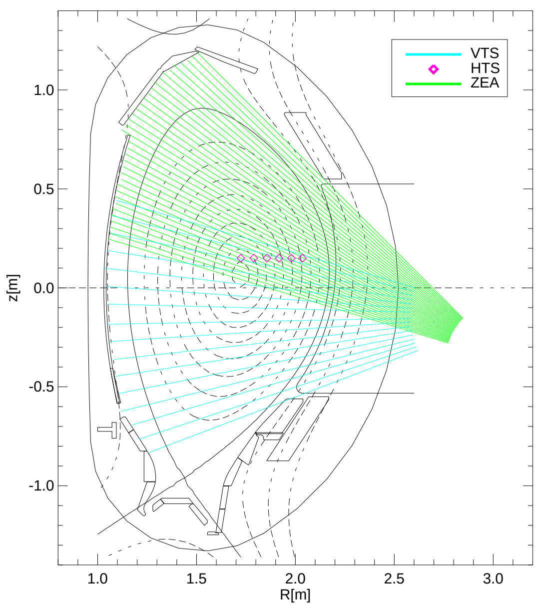

***Figure 1:** Projection of the sight-lines of the Z_{eff} diagnostic at ASDEX Upgrade into a poloidal cross-section.*

The deconvolution procedure The usage of sight-lines in poloidal and toroidal direction at varying wavelengths together with the measurement in an elongated plasma without up-down symmetry requires a generally applicable deconvolution algorithm. The algorithm adopted is based on the matrix inversion method and uses curvature minimization as regularization. The functional to be minimized is given by

$$F = \sum_{j=1}^{N_{sp}-1} w_j \int_{\rho_j}^{\rho_{j+1}} \left(\frac{\partial^2 \varepsilon(\rho)}{\partial \rho^2} \right)^2 d\rho + A \cdot \sum_{i=1}^{N_{SL}} \left(\frac{B_i - I_i}{\Delta B_i \cdot B_i} \right)^2 \tag{1}$$

when representing the resulting profile ε by a cubic spline over the normalized minor radius. The first term expresses the minimization of the curvature with w_j being the weighting factors for each interval of the N_{sp} spline knots ρ_j. The second gives the deviation of the measured bremsstrahlung emissivity B_i of each of the N_{SL} sight-lines (in units of $\frac{W}{m^2 st}$) from the calculated sight-line integral I_i when taking the current spline representation into account. The deviations should be of the order of the relative error ΔB_i of the measurement. Therefore the weighting factor A between curvature and chi-square part is changed by a factor of $\frac{\chi^2}{N_{SL}}$ for each iteration until either A or χ^2 do not change further.

The measured emissivity of bremsstrahlung is given by the sight-line integral over the power of the emitted bremsstrahlung per unit wavelength, volume and solid angle:

$$\begin{aligned} B_i &= \int_{SL} dl \int_0^{\infty} d\lambda \frac{d^3 P_\lambda}{d\lambda dV d\Omega} \\ &= \int_{SL} dl \int_0^{\infty} d\lambda \; C \cdot \bar{g}_{\text{eff}} \frac{n_e^2 Z_{\text{eff}}}{\sqrt{k_B T_e}} \frac{\exp\left(-\frac{hc}{\lambda k_B T_e}\right)}{\lambda^2} T_i(\lambda) \end{aligned} \tag{2}$$

with all the physical constants merged into $C = \frac{1}{4\pi} \frac{e^6}{(4\pi\epsilon_0)^3} \frac{16}{3} \sqrt{\frac{2\pi m_e}{3}} \frac{2\pi c}{m_e^2 c^3}$. The second integration over the wavelength λ takes the transmission $T_i(\lambda)$ of the filters into account; $\bar{g}_{\text{eff}}$ is the effective Gaunt-factor calculated according to [2].

With the definition of a weighted length matrix for discrete knots along each sight-line

$$L_{ij} = C \cdot \bar{g}_{\text{eff}} \frac{n_e^2}{\sqrt{k_B T_e}} \tag{3}$$

and writing the sight-line integral as a discrete sum one arrives at

$$I_i = \sum_j L_{ij} Z_{\text{eff}\,j} \tag{4}$$

with i being the index of the sight-line and j the index of the spline knot. Inserting equation (4) into the functional (1) gives the Z_{eff}-profile as result of the deconvolution represented in a spline basis with arbitrary spline knots and individual curvature weighting of the spline intervals. In order to ease the convergence of the algorithm, the factor $\frac{\exp\left(-\frac{hc}{\lambda k_B T_e}\right)}{\lambda^2} T_i(\lambda)$ is used to normalize the measured emissivities of each sight-line under the assumption that the exponential function does not change very much along the respective sight-line (which is given within 3% apart from the edge points where T_e approaches zero).

The reason for choosing this approach to the calculation of Z_{eff} rather than the common one of deconvoluting first a profile of the bremsstrahlung emissivity and using this to calculate Z_{eff},

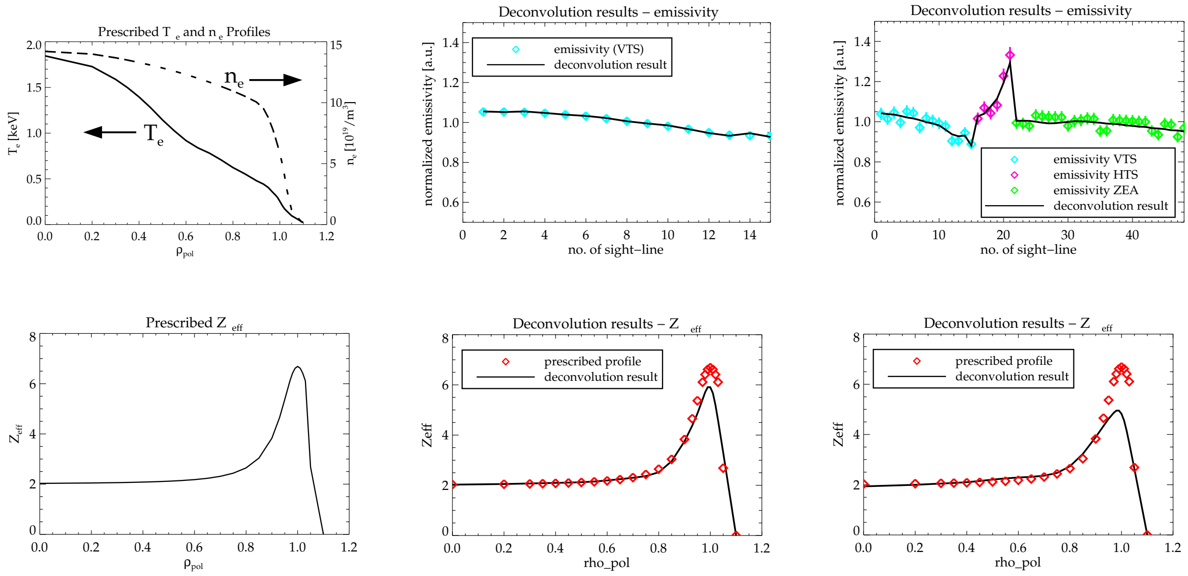

(a) Prescribed T_e, n_e (top) and Z_{eff}-profiles (bottom) for testing the deconvolution procedure.

(b) Ideal bremsstrahlung emissivities of the sight-lines of VTS according to 2(a) (top) and the reproduced Z_{eff} profile (bottom).

(c) Bremsstrahlung emissivities according to 2(a) with added random noise for all sight-lines (top) and the reproduced Z_{eff} profile (bottom).

Figure 2: *Test of the deconvolution procedure.*

is that the Gaunt-factor varies along each sight-line and changes from sight-line to sight-line, depending on the wavelength of the respective filters. Therefore it is not possible to define one profile for $\bar{g}_{\mathrm{eff}}$ over ρ_{pol} for all the different sight-lines.

The deconvolution procedure was tested using assumed T_e, n_e and Z_{eff}-profiles (see figure 2(a)). T_e and n_e profiles are typical for ASDEX Upgrade H-mode discharges; the rather strong peak of Z_{eff} around the separatrix was assumed in order to show that the deconvolution procedure is capable of reproducing even such features. The expected bremsstrahlung emissivities as expected from these values were used as input to the deconvolution procedure. Figure 2(b) shows that the algorithm is able to reproduce the assumed Z_{eff}-profile when providing ideal values for the sight-line integrated ”measurements”. This still remains true when random noise is added to the ”measured” emissivities and all the sight-lines measuring bremsstrahlung are considered, as the results of figure 2(c) prove.

First results Applying the deconvolution routine to the Z_{eff} measurements of an improved H-mode of ASDEX Upgrade gives the profile shown in figure 3. It seems to be slightly peaked in the center and has also the strong increase of Z_{eff} around the separatrix. The deconvolution of an H-mode with high triangularity using VTS and ZEA sight-lines results in a rather flat Z_{eff} profile in the plasma core which increases towards the edge. A comparison of the measured sight-line emissivities of both shown disharges with the ”ideal” ones of figure 2(b) reveals that the measurement is strongly affected by noise and that the assumed relative errors may be underestimated. Furthermore, due to technical problems the absolute calibration of the system is inaccurate, as can be seen from the deviations of sight-lines 3

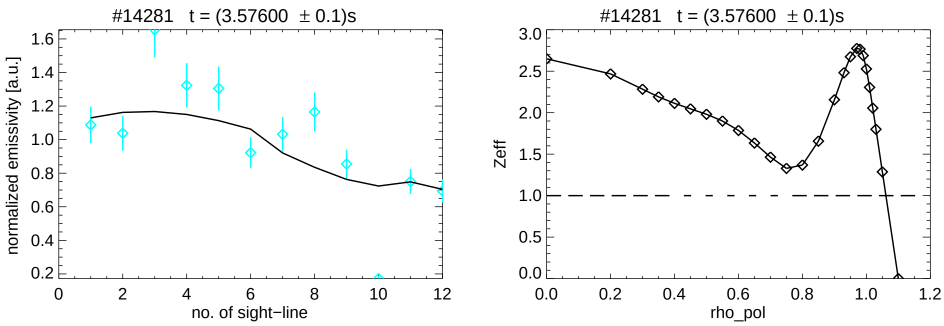

Figure 3:*First result of the deconvolution of an improved H-mode (#14281, $t = 3.55\,s$).*

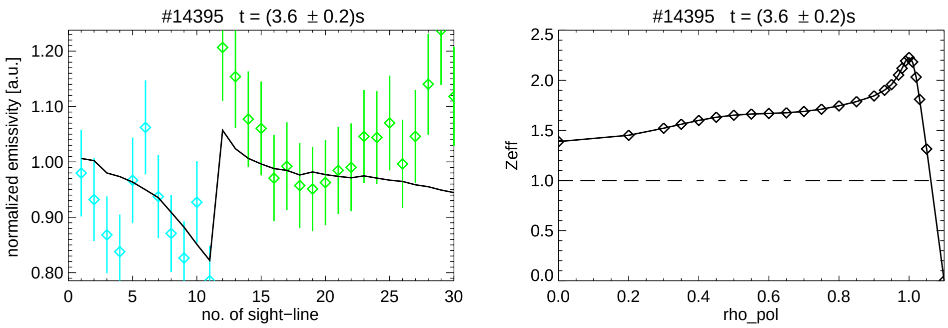

Figure 4: *First result of the deconvolution of an H-mode with high triangularity, $\delta \approx 0.4$, using VTS (blue) and ZEA (green) sight-lines (#14395, $t = 3.6\,s$).*

and 10 in figure 3 and those between VTS and ZEA sight-lines in figure 4. A re-calibration during the next maintenance period will reduce the uncertainties.

Diagnostic extensions underway The Z_{eff} diagnostic at ASDEX Upgrade is undergoing an extension which will not only provide new sight-lines, but give more insight into the bremsstrahlung emissivity and its evaluation in terms of a Z_{eff}-profile. The reason for this extension is that previous measurements, especially the ones using VTS sight-lines, suffered frequently from thermal radiation from the inner heat shield during high power discharges or from impurity line radiation.

First, the measurement will be done spectroscopically, i.e. using a spectrometer and a CCD-camera as detector for observing the bremsstrahlung. This technique allows the measurement in different wavelength ranges across the whole visible spectrum and up to 1080 *nm* (depending on the sensitivity of the system) knowing exactly if there is line emission in the observed range or not.

Second, the geometrical arrangement of the sight-lines is optimized for the observation of the region around the separatrix in the outer mid-plane, but also providing two sight-lines looking through the plasma core. The latter two will be used mainly for monitoring the bremsstrahlung spectra in the core whereas 12 sight-lines will cover the boundary and give a spatial resolution of about 1 *cm*. These will be used for reducing the uncertainties in the Z_{eff}-profile in the region of high density and temperature gradients, the region which determines the confinement properties of the operating scenario chosen for ITER.

References

[1] Röhr *et al.*, Review of Scientific Instruments **59**, 1875 (1988).

[2] W. J. Karzas and R. Latter, Astrophysical Journal — Supplement Series **6**, 167 (1961).